

**CORROSION MONITORING OF GALVANIZED STEEL UNDER CHLORIDE  
RICH ENVIRONMENT USING POTENTIOSTAT TESTING**

**NURAMIRA BINTI AZMAN**

**This report is submitted  
in fulfilment of the requirements for the degree of  
Bachelor of Mechanical Engineering**

**Faculty of Mechanical Engineering**

**UNIVERSITI TEKNIKAL MALAYSIA MELAKA**

**2021**

## DECLARATION

I declare that this project report entitled “Corrosion Monitoring of Galvanized Steel Under Chloride Rich Environment Using Potentiostat Testing” is the result from my own work except as cited in the references.

Signature : .....

Name : .....

Date : .....

## **APPROVAL**

I hereby declare that I have read this project report and in my opinion this report is sufficient in terms of scope and quality for the award of the Degree of Bachelor of Mechanical Engineering.

Signature : .....

Name : .....

Date : .....

## **DEDICATION**

I would like to dedicate my report to my beloved mother and father.

Thank you for always believing in me.

## ABSTRACT

Corrosion monitoring of galvanized steel (GS) is very crucial as it is one of the most widely used metals in the industry such as the oil and gas industry, where most of the critical pipelines are made of GS. This project was to study the corrosion behaviour of GS when exposed to chloride rich environment. In this study, sodium chloride (NaCl) solution was used to replicate the chloride rich environment. Three different concentration of NaCl solution which are 0.3 M, 0.5 M and 1.0 M and potentiostat testing was used to accelerate the corrosion process. The samples were prepared according to the standard ASTM G59-97. The samples were immersed in the 0.3 M, 0.5 M and 1.0 M NaCl solution at normal room temperature from 20 °C to 25 °C with a potential range of -0.5 V to 0.5 V and the scan rate of 0.5 mV/s. The immersion time was set to one hour for each concentration. The electrochemical region during the corrosion process of GS was studied from the potentiodynamic curve obtained. Furthermore, from the potentiodynamic curve, the corrosion potential ( $E_{\text{corr}}$ ), corrosion current density ( $i_{\text{corr}}$ ) and corrosion rate (CR) of GS were determined from the Tafel curve generated. The experimental results revealed that the sample of GS had the highest CR when immersed in 1.0 M NaCl solution while the lowest CR occurred in 0.3 M NaCl solution. Moreover, the surface morphology of the GS samples before and after the immersion was analysed using Scanning Electron Microscopy (SEM). The SEM analysis confirmed that the pit holes formed at the GS samples after the immersion in NaCl solution. The size of pit holes of the GS sample in 1.0 M NaCl solution was averagely larger compared to 0.3 M and 0.5 M NaCl solution. The SEM analysis proved that GS exposed to chloride rich environment was severely affected by corrosion.

## ABSTRAK

*Pemantauan kakisan keluli tergalvani (GS) sangat penting kerana GS adalah salah satu logam yang paling banyak digunakan dalam industri seperti industri minyak dan gas, di mana kebanyakan saluran paip kritikal diperbuat dari GS. Projek ini bertujuan untuk mengkaji pemantauan kakisan GS apabila terdedah kepada persekitaran yang kaya dengan klorida. Dalam kajian ini, larutan natrium klorida (NaCl) digunakan untuk menggantikan persekitaran yang kaya dengan klorida. Tiga larutan natrium klorida dengan kepekatan yang berbeza iaitu 0.3 M, 0.5 M dan 1.0 M dan pengujian potentiostat digunakan untuk mempercepat proses pengaratan. Sampel disediakan mengikut piawaian ASTM59-97. Sampel direndam di dalam larutan NaCl dalam 0.3 M, 0.5 M dan 1.0 M pada suhu bilik normal iaitu dari 20 °C hingga 25 °C dengan lingkungan potensi -0.5 V hingga 0.5 V dan kadar imbasan 0.5 mV/s. Masa rendaman ditetapkan ialah satu jam untuk setiap kepekatan dan sampel. Kawasan elektrokimia semasa proses pengaratan GS dikenal pasti berdasarkan lengkung potentiodynamik yang diperolehi. Selanjutnya, dari lengkung potentiodynamik tersebut, potensi kakisan ( $E_{corr}$ ), ketumpatan arus kakisan ( $i_{corr}$ ) dan kadar kakisan (CR) GS dapat ditentukan dari lengkung Tafel yang dijanakan. Hasil eksperimen menunjukkan bahawa sampel GS mempunyai CR tertinggi ketika direndam dalam larutan NaCl 1.0 M sementara itu, CR terendah diperhatikan dalam 0.3 M larutan NaCl. Tambahan pula, morfologi permukaan sampel GS sebelum dan selepas perendaman dianalisis menggunakan Microskop Elektron Imbasan (SEM). Analisis SEM mengesahkan bahawa lubang pit yang terbentuk pada sampel GS setelah rendaman dalam larutan NaCl. Ukuran lubang pit sampel GS dalam 1.0 M larutan NaCl menunjukkan lubangnya lebih besar berbanding larutan NaCl 0.3 M dan 0.5 M larutan NaCl. Analisis SEM membuktikan bahawa GS yang terdedah kepada persekitaran yang kaya dengan klorida sangat terjejas teruk oleh kakisan.*

## ACKNOWLEDGEMENTS

First and foremost, I would like to praise Allah the Almighty for His guidance. With His guidance and blessing bestowed upon me, I managed to overcome all obstacles in completing this project. Here, I would like to use this special opportunity to express my heartfelt gratitude to everyone that has contributed to the success of the project.

My deepest appreciation and gratitude to my supervisor, Dr Zakiah Abd Halim from Faculty of Mechanical Engineering for her supervision, commitment, professionalism, advice and guidance throughout the completion of my project.

Particularly, I would like to extend my deepest gratitude to Miss Adibah, the assistant lab from the chemistry lab and Mr Mahader, the technicians from Scanning Electron Microscopy (SEM) lab Faculty of Mechanical Engineering.

Special thanks to all my peers, mother, father and siblings for their moral support in completing this project. Last but not least, special thanks to those who helped me directly or indirectly in undertaking this project throughout the year. The contributions and insights are highly appreciated.

## TABLE OF CONTENT

<b>DECLARATION</b>	
<b>DEDICATION</b>	
<b>ABSTRACK</b> .....	i
<b>ABSTRAK</b> .....	ii
<b>ACKNOWLEDGEMENTS</b> .....	iii
<b>TABLE OF CONTENT</b> .....	iv
<b>LIST OF TABLES</b> .....	vi
<b>LIST OF FIGURES</b> .....	vii
<b>LIST OF ABBREVIATIONS</b> .....	ix
<b>CHAPTER 1 INTRODUCTION</b> .....	1
1.1 Background of study.....	1
1.2 Problem statement.....	2
1.3 Objectives.....	3
1.4 Scope.....	3
<b>CHAPTER 2 LITERATURE REVIEW</b> .....	4
2.1 Types of corrosion.....	4
2.2 Factors influencing corrosion.....	8
2.3 Corrosion process.....	14
2.4 Electrochemical monitoring technique.....	17



<b>CHAPTER 3 METHODOLOGY</b> .....	28
3.1 Flow chart.....	28
3.2 Sample preparation.....	29
3.3 Surface preparation.....	31
3.4 Solution preparation.....	31
3.5 Electrochemical setup.....	33
3.6 Surface morphology.....	39
<b>CHAPTER 4 RESULT AND DISCUSSION</b> .....	40
4.1 Corrosion behaviour of GS.....	40
4.2 Potentiodynamic curve.....	42
4.3 Tafel plot.....	58
4.4 SEM analysis.....	61
<b>CHAPTER 5 CONCLUSION AND RECOMMENDATION</b> .....	70
<b>REFERENCES</b> .....	72

## LIST OF TABLES

Table 2.1: SEM images of corrosion attack on AISI 1040 (Ismail & Adan, 2014) .....	12
Table 2.2: Summary of previous study .....	19
Table 2.3: Parameters resulted from potentiodynamic polarization curves (Li et al., 2020) .....	23
Table 2.4: Corrosion potential and current density for bare sample, MS, SH and SH@MS in 3.5 wt% NaCl solution (Li et al., 2020) .....	24
Table 3.1: List of the GS sample used in this project.....	29
Table 3.2: Mass of crystallized NaCl required for 0.3 M, 0.5 M and 1.0 M NaCl solution	32
Table 3.3: Connection of the electrode to Gamry Reference 600 (Potentiostat mode) .....	36
Table 4.1: Value of $E_{\text{corr}}$ , $i_{\text{corr}}$ and CR of GS.....	58
Table 4.2: Pit hole size of GS in 0.3 M, 0.5 M and 1.0 M NaCl solution .....	69

## LIST OF FIGURES

Figure 2.1: Uniform corrosion on disc coupon (Mansoori et al., 2017).....	5
Figure 2.2: Pitting corrosion at internal surface of pipeline (Mansoori et al., 2017) .....	6
Figure 2.3: Intergranular corrosion of GS buried in black clay (Karthick et al., 2020) .....	7
Figure 2.4: SEM images of CS specimen that was coupled to SS316 at A) 100X, B) 500X and C) 1000X magnification (Farhan & Abraham, 2019).....	7
Figure 2.5: Electrochemical series (Zaki, 2006).....	8
Figure 2.6: AISI 1040 in 3.5 wt% NaCl solution (Ismail & Adan, 2014).....	10
Figure 2.7: AISI 1040 in H <sub>2</sub> SO <sub>4</sub> (Ismail & Adan, 2014).....	10
Figure 2.8: AISI 1040 in HCl solution (Ismail & Adan, 2014).....	11
Figure 2.9: CR of AISI 1040 in all solutions (Ismail & Adan, 2014).....	11
Figure 2.10: Critical CR of all solutions (Ismail & Adan, 2014) .....	12
Figure 2.11: CR over time for pH 4.0 (Tanupabrungsun et al., 2013).....	13
Figure 2.12: CR over time for pH 6.0 (Tanupabrungsun et al., 2013).....	14
Figure 2.13: Schematic diagram of corrosion process (Zaki, 2006).....	15
Figure 2.14: The flow of electrons (Zaki, 2006).....	16
Figure 2.15: The formation of corrosion (rust) (Zaki, 2006) .....	16
Figure 2.16: : Potentiodynamic polarization for bare sample, MS, SH and SH@MS in....	24

Figure 2.17: SEM of GS (a) before corrosion; after corrosion in (b) 5% NaCl solution; (c) seawater and (d) rainwater. All corrosion test was immersed for 5 days (Merajul Haque et al., 2014).....	25
Figure 2.18: Weight loss of GS in HCl (Mohamod, Kasim, 2014) .....	26
Figure 2.19: Weight loss of GS in H <sub>2</sub> SO <sub>4</sub> (Mohamod, Kasim, 2014) .....	26
Figure 2.20: Weight loss of GS in HNO <sub>3</sub> (Mohamod, Kasim, 2014) .....	27
Figure 3.1: Flow chart.....	28
Figure 3.2: Dimension of GS .....	30
Figure 3.3: Shearing cutting machine .....	30
Figure 3.4: 240 and 600 grit sandpaper (SiC).....	31
Figure 3.5: Digital Analytical Balance.....	32
Figure 3.6: Gamry Ag/AgCl Reference .....	33
Figure 3.7: Graphite rod.....	34
Figure 3.8: Round polystyrene is used in corrosion experiment .....	35
Figure 3.9: Corrosion cell of experiment.....	35
Figure 3.10: Gamry's Reference 600.....	36
Figure 3.11: Standard cell cable .....	37
Figure 3.12: Electrode connections.....	38
Figure 3.13: Experimental setup for potentiodynamic test.....	38
Figure 3.14: SEM software .....	39
Figure 3.15: GS in SEM.....	39
Figure 4.1: Illustration of corrosion behaviour of GS .....	41
Figure 4.2: Potentiodynamic curve of GS (9.2 cm <sup>2</sup> ) in 0.3 M NaCl solution.....	43
Figure 4.3: Potentiodynamic curve of GS (9.2 cm <sup>2</sup> ) in 0.5 M NaCl solution.....	45
Figure 4.4: Potentiodynamic curve of GS (9.2 cm <sup>2</sup> ) in 1.0 M NaCl solution.....	47

Figure 4.5: Potentiodynamic curve of GS (18 cm <sup>2</sup> ) in 0.3 M NaCl solution.....	49
Figure 4.6: Potentiodynamic curve of GS (18 cm <sup>2</sup> ) in 0.5 M NaCl solution.....	51
Figure 4.7: Potentiodynamic curve of GS (18 cm <sup>2</sup> ) in 1.0 M NaCl solution .....	53
Figure 4.8: Potentiodynamic curve of GS (9.2 cm <sup>2</sup> ) in 0.3 M, 0.5 M and 1.0 M NaCl solution .....	55
Figure 4.9: Potentiodynamic curve of GS (18 cm <sup>2</sup> ) in 0.3 M, 0.5 M and 1.0 M NaCl solution .....	56
Figure 4.10: Tafel curve of GS (9.2 cm <sup>2</sup> ) in 0.3 M, 0.5 M and 1.0 M NaCl solution.....	59
Figure 4.11: Tafel curve of GS (18 cm <sup>2</sup> ) in 0.3 M, 0.5 M and 1.0 M NaCl solution.....	60
Figure 4.12: SEM image of GS before immersed in NaCl solution .....	61
Figure 4.13: SEM image of GS (9.2 cm <sup>2</sup> ) after immersed in 0.3 M NaCl solution .....	62
Figure 4.14: SEM image of GS (18 cm <sup>2</sup> ) after immersed in 0.3 M NaCl solution.....	62
Figure 4.15: SEM image of GS (9.2 cm <sup>2</sup> ) after immersed in 0.5 M NaCl solution.....	63
Figure 4.16: SEM image of GS (18 cm <sup>2</sup> ) after immersed in 0.5 M NaCl solution.....	63
Figure 4.17: SEM image of GS (9.2 cm <sup>2</sup> ) after immersed in 1.0 M NaCl solution.....	64
Figure 4.18: SEM image of GS (18 cm <sup>2</sup> ) after immersed in 1.0 M NaCl solution .....	64
Figure 4.19: Pit holes size of GS (9.2 cm <sup>2</sup> ) after immersed in 0.3 M NaCl solution.....	65
Figure 4.20: Pit holes size of GS (9.2 cm <sup>2</sup> ) after immersed in 0.5 M NaCl solution.....	66
Figure 4.21: Pit holes size of GS (9.2 cm <sup>2</sup> ) after immersed in 1.0 M NaCl solution.....	66
Figure 4.22: Pit holes size of GS (18 cm <sup>2</sup> ) after immersed in 0.3 M NaCl solution.....	67
Figure 4.23: Pit holes size of GS (18 cm <sup>2</sup> ) after immersed in 0.5 M NaCl solution.....	68
Figure 4.24: Pit holes size of GS (18 cm <sup>2</sup> ) after immersed in 1.0 M NaCl solution.....	68

## LIST OF ABBREVIATIONS

ABS	Ammonium Bisulfide Solution
AFM	Atomic Force Microscopy
Ag/AgCl	Silver/silver chloride
Al	Aluminium
Au	Gold
BC	Black clay
Cl <sup>-</sup>	Chloride ion
CR	Corrosion rate
CS	Carbon steel
Cu/CuSO <sub>4</sub>	Copper/copper sulphate
EIS	Electrochemical Impedance Spectroscopy
E <sub>corr</sub>	Corrosion potential
Fe	Iron
Fe(OH) <sub>2</sub>	Ferrous hydroxide
FT-IR	Fourier-Transform Infrared
GS	Galvanized steel
HCl	Hydrochloric acid
HDG	Hot dip galvanized steel
HNO <sub>3</sub>	Nitric acid
H <sub>2</sub> SO <sub>4</sub>	Sulfuric acid
i <sub>corr</sub>	Corrosion current density
KCl	Potassium chloride
MS	Mild steel
NaCl	Sodium chloride
OH <sup>-</sup>	Hydroxyl ion
Pt	Platinum

SCC	Stress corrosion cracking
SCE	Saturated calomel electrode
SEM	Scanning Electron Microscopy
SHE	Standard hydrogen electrode
SS	Stainless steel
SiC	Silicon carbide
XRD	X-Ray Diffractometer
XPS	X-Ray Photoelectron Spectrometer
$V_f$	Potential
WC	White clay

## CHAPTER 1

### INTRODUCTION

#### 1.1 Background of study

Corrosion is one of the major challenges to the durability of assets in any process-intensive industry that uses volatile materials such as in the oil and gas or petrochemicals industry. Oil and gas industry contains equipment such as boilers or pressure vessels will slowly wear down due to corrosion without proper monitoring which can be causing leaks or failures and leading to poor performance and reliability. In severe situations, if corrosion is left unmonitored, it can lead to complete breakdown, catastrophic failure, posing safety hazards to staff, tremendous costs of machinery and resulting harm to the environment.

Corrosion monitoring is a process that evaluates and monitors equipment components, structure, process units and facilities to detect the early stage of corrosion. In order to overcome the catastrophic failure and unplanned downtime of the structure, corrosion monitoring must be carried out by ensuring the availability and reliability of the structure. Hence, can minimizing breakdown maintenance and extend the lifespan of the property.

Zinc and its alloy have been commonly used to prolong the life of steel structures by cathodic protection as a corrosion protection coating. For many applications, galvanizing is a good option to extend the lifetime of structure such as electricity, transportation, communication, harbor facilities due to the excellent anti-corrosion performance of zinc coating. The galvanized layer gives the steel substrate effective corrosion resistance when



exposed to the environment. However, zinc is relatively lively and easy to be corroded, especially in moist and aggressive environment. Corrosive environment such as seawater environments can accelerate zinc corrosion, which fails to offer sufficient protection for steel substrate against corrosion. In order to replicate the seawater environment, sodium chloride (NaCl) solution is used in this experiment. Hence, monitoring the corrosion due to NaCl solution is studied in this project.

## **1.2 Problem statement**

Corrosion is one of the most well-known phenomena in the oil and gas industry yet most difficult to prevent corrosion from occurring. Therefore, various factor effect of corrosion on galvanized steel (GS) in chloride rich environment is the concentration of NaCl, concentration of oxygen, electrochemical potential and surrounding temperature. Several experiments have been carried out over the past ten years to track or detect pipeline corrosion made of different types of materials such as mild steel (MS), stainless steel (SS) and carbon steel (CS) by using electrochemical measures such as potentiodynamic polarization, Tafel plot and Scanning Electron Microscopy (SEM) method. However, there are lesser studies had been done on GS. Therefore, this project of GS exposed to NaCl solution is conducted to understand the corrosion rate and to observe the corrosion process of GS.

In this case study, the GS was exposed to the chloride rich environment which is NaCl solution. NaCl solution contain chloride ion ( $\text{Cl}^-$ ) which is corrosive in nature. This is due to the real case situations, the substrates come into contact with liquid and gases such as chemical processing plants, plumbing applications, offshore petroleum pipelines, roofing sheets, machine components and marine structure (Merajul Haque et al., 2014). The relative corrosion performance is monitored through potentiodynamic polarization and Tafel plot.

All the experiments were carried out at an exposure period of one hour. The surface morphology before and after the exposure was verified with SEM method.

### **1.3 Objectives**

The objectives of these projects are:

1. To investigate the effect of different concentration on GS.
2. To examine the corrosion behaviour of different surface area of GS.
3. To determine the size of pitholes of GS when subjected to the different concentration of corrosive environment.

### **1.4 Scope**

The scope of this project focuses on the corrosion monitoring of pipeline through laboratory experiment. The GS sample was used to simulate the practical use of pipeline and exposed to chloride rich environment. The chloride rich environment was replicated using NaCl solution with different concentration which are 0.3 M, 0.5 M and 1.0 M. The corrosion process was accelerated using Gamry's Reference 600 potentiostat and the relative corrosion performance is monitored through potentiodynamic curve. Next, the different exposed area of GS. Lastly, the surface morphology before and after the exposure was characterized by using SEM method to verify the corrosion activity.

## CHAPTER 2

### LITERATURE REVIEW

#### 2.1 Types of corrosion

Corrosion is defined as the destruction or degradation of materials because of exposure or reaction to an environment which is restricted to metals and non-metals (Yahaya et al., 2019). Corrosion attacks infrastructures such as bridges, pipelines, vehicles, utilities (electrical, telecommunications and nuclear power plant), engineering and manufacturing, chemical industry and the oil and gas industry (International et al., 2017). However, when focusing on the pipeline in the oil and gas industry, corrosion can occur at the external and internal surfaces of the pipeline.

Various types of corrosion happened to pipeline and also other structure such as pitting corrosion (Darband et al., 2016; Jiang et al., 2019; Krawczyk et al., 2017; Mansoori et al., 2017; Nakhaie et al., 2020; Rashad et al., 2016), uniform corrosion (Jiang et al., 2019; Krawczyk et al., 2017; Mansoori et al., 2017; Tittarelli et al., 2018), stress corrosion cracking (SCC) (Ryakhovskikh et al., 2018) crevice corrosion (Rashad et al., 2017), galvanic corrosion (Dong et al., 2010; Farhan & Abraham, 2019; Gao et al., 2018; García-Rodríguez et al., 2019; Ha et al., 2018; Shaika & Thamidab, 2019) and intergranular corrosion (Karthick et al., 2020; Srinivasan et al., 2014).

Uniform corrosion is also known as general corrosion that refers to corrosion that occurs on the metal surface uniformly. In other words, the corrosion on the entire metal surface is exposed to the corrosive environment at the same rate. In uniform corrosion, it is

not possible to differentiate between anodes or cathodes that randomly emerging because of the electrochemical process. The most common example of uniform is iron rusting which occurs as a result of oxidation of the iron metal. Figure 2.1 shows the uniform corrosion on the disc coupon that was used in the study by Mansoori et al. (2017). This study is to monitored the uniform corrosion internal part of wet gas pipelines. The coupons were in service for 3 to 6 months at the wellhead facilities and then were recovered for weight-loss testing.



Figure 2.1: Uniform corrosion on disc coupon (Mansoori et al., 2017)

Pitting is the most destructive type of corrosion, as it can be difficult to predict, detect and characterize (U.S. Naval Academy, 2003). It generally appears first as small white or grey dots and grows into a hole or cavity that takes on one of a variety of different shapes. The metal surface itself may be caused by non-uniformities. Pitting corrosion is localized accelerated metal dissolution resulting from the degradation of the protective passive layer on the surface of the metal. What makes it even more dangerous is that the pits are often not apparent because they are hidden by corrosion materials, but the corrosion continues to

perforate the metal surface. Therefore, continuous pitting corrosion monitoring is extremely important for the integrity of the metal. Similar study by Mansoori et al. (2017), showing that the pitting corrosion found at the internal surface of a wet gas pipeline as shown in Figure 2.2. The failure location is marked in the main pit that occurs on the surface of the pipe and the shallower pit is located near the main pit.



Figure 2.2: Pitting corrosion at internal surface of pipeline (Mansoori et al., 2017)

Intergranular corrosion is a chemical or electrochemical attack on the grain boundaries of metal. Higher contents of effects near to the grain boundaries occur due to impurities in the metal. Intergranular corrosion is also called intercrystallite corrosion or interdendritic corrosion. The study by Karthick et al. (2020) on the microstructure of the intergranular corrosion was shown in Figure 2.3. In this study, GS was buried in black clay (BC) after 90 days of exposure. With increasing the magnification, the GS surface has shown a cracked zinc layer and intergranular corrosion running along the grain boundaries.

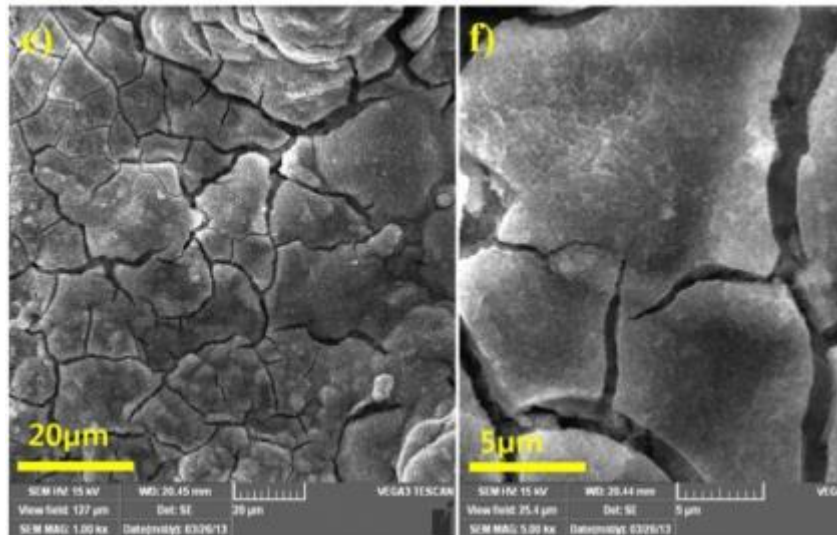


Figure 2.3: Intergranular corrosion of GS buried in black clay (Karthick et al., 2020)

Galvanic corrosion is also called bimetallic corrosion (Baboian & Begum, 2016). Galvanic corrosion takes place when two different metals are being in electrical contact with each other in the presence of an electrolyte which is one metal acts as an anode and another metal as a cathode (Farhan & Abraham, 2019). The electro potential difference between two electrode reactions is the driving force that dissolves into the electrolyte for an accelerated assault on anode metal. This allows the metal to corrode more rapidly at the anode than it would otherwise and corrosion at the cathode being inhibited. Figure 2.4 below shows the SEM image of CS coupled with SS316 in 3.5 wt% NaCl solution at room temperature. SEM image shows that the CS suffered galvanic corrosion on rough surface with deep pits on it.

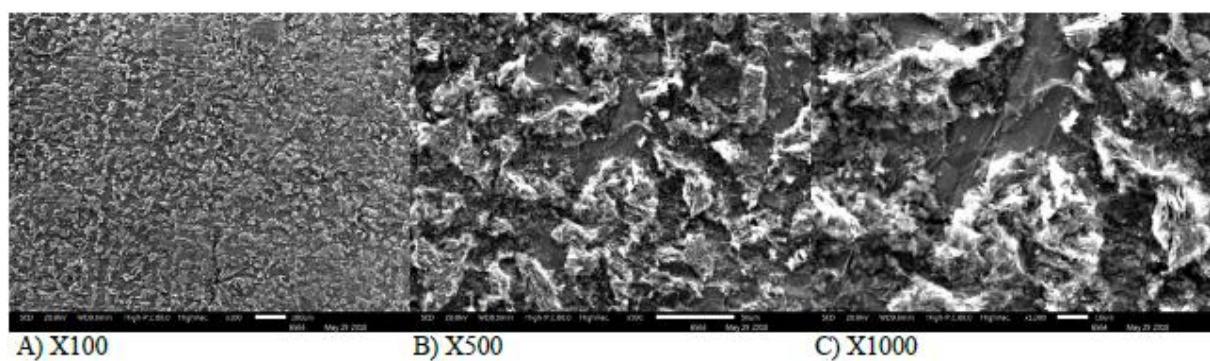


Figure 2.4: SEM images of CS specimen that was coupled to SS316 at A) 100X, B) 500X and C) 1000X magnification (Farhan & Abraham, 2019)

## 2.2 Factors influencing corrosion

The rate of corrosion of the metal can be influenced by few factors (Karthick et al., 2020; Marcus, 2011; Orlikowski et al., 2017) which are the position of the metal in the electrochemical series (Zaki Ahmad, 2006), the concentration of electrolyte (Chu et al., 2019), oxygen concentration (Ismail & Adan, 2014), pH of environment and temperature of the environment (Tanupabrungsun et al., 2013).

Firstly, the factors influencing corrosion is the position of metal in the electrochemical series. The position of the metal in the electrochemical series decides the rate of corrosion as shown in Figure 2.5. More reactive metals have a greater tendency to lose an electron and corrode more easily. For example, iron metal (Fe) is more reactive than gold metal (Au) because Fe will readily give up electrons to oxygen while Au will not. Due to more reactivity, Fe metal will corrode more quickly than Au to form rust.

Electrode reaction	$E^\circ$ (V)
$\text{Au}^{+3} + 3e = \text{Au}$ .....	1.50
$\text{Pt}^{++} + 2e = \text{Pt}$ .....	ca 1.2
$\text{Hg}^{++} + 2e = \text{Hg}$ .....	0.854
$\text{Pd}^{++} + 2e = \text{Pd}$ .....	0.987
$\text{Ag}^+ + e = \text{Ag}$ .....	0.800
$\text{Hg}_2^{++} + 2e = 2\text{Hg}$ .....	0.789
$\text{Cu}^+ + e = \text{Cu}$ .....	0.521
$\text{Cu}^{++} + 2e = \text{Cu}$ .....	0.337
$2\text{H}^+ + 2e = \text{H}_2$ .....	0.000
$\text{Pb}^{++} + 2e = \text{Pb}$ .....	-0.126
$\text{Sn}^{++} + 2e = \text{Sn}$ .....	-0.136
$\text{Mo}^{+3} + 3e = \text{Mo}$ .....	ca -0.2
$\text{Ni}^{++} + 2e = \text{Ni}$ .....	-0.250
$\text{Co}^{++} + 2e = \text{Co}$ .....	-0.277
$\text{Tl}^+ + e = \text{Tl}$ .....	-0.336
$\text{In}^{+3} + 3e = \text{In}$ .....	-0.342
$\text{Cd}^{++} + 2e = \text{Cd}$ .....	-0.403
$\text{Fe}^{++} + 2e = \text{Fe}$ .....	-0.440
$\text{Ga}^{++} + 3e = \text{Ga}$ .....	-0.53
$\text{Cr}^{+3} + 3e = \text{Cr}$ .....	-0.74
$\text{Zn}^{++} + 2e = \text{Zn}$ .....	-0.763
$\text{Nb}^{+3} + 3e = \text{Nb}$ .....	ca -1.1
$\text{Mn}^{++} + 2e = \text{Mn}$ .....	-1.18

Figure 2.5: Electrochemical series (Zaki, 2006)

Secondly, the concentration of electrolyte used which is NaCl solution. Research by He Juan (2010) about the corrosion of chloride ions in metal solutions in aqueous solution. It was found that  $\text{Cl}^-$  in aqueous solutions could destroy the passivation film of metal in the process of competing in the absorption process with hydrogen and oxygen ions. This led to the occurrence of pitting corrosion, hole corrosion and crevice corrosion and made the metal equipment more sensitive to corrosion. Furthermore, to expand the study, research by Hornous (2015) studied the effect of  $\text{Cl}^-$  on the crevice corrosion of aluminium alloy. It was found that when the  $\text{Cl}^-$  concentration increase, the corrosion rate of the aluminium alloy also increases. Therefore, Ma Yunlin (2017), showed that the increase of  $\text{Cl}^-$  concentration in the solution, the pitting potential of stainless steel decreased, while the blunt current density became larger. It indicated that the metal was more prone to crevice corrosion with increasing  $\text{Cl}^-$  concentration. Form this research, it shows that the high concentration of  $\text{Cl}^-$  greatly affected the performance of the metal.

Furthermore, the oxygen concentration will affect the corrosion rate of the metal. The higher concentration of oxygen, it will quickly increase the corrosion rate (CR) of the metal. Therefore, if the metal is exposed to high concentration of oxygen, it will corrode faster than the metal that exposes less concentration of oxygen. Previous studies on oxygen concentration content effect the corrosion have found that the corrosion rate is higher when the material is exposed in solutions with oxygen content (Ismail & Adan, 2014). The researchers carried out an experiment on CS with AISI 1040 to studied the effect of oxygen concentration on CR of AISI 1040 in NaCl,  $\text{H}_2\text{SO}_4$  and HCl. Figure 2.6 shows the result of anodic and cathodic polarization of CS in 3.5 wt% NaCl with and without oxygen content whereas Figure 2.7 and Figure 2.8 present the potentiodynamic curve behaviour of AISI 1040 in  $\text{H}_2\text{SO}_4$  and HCl solutions, respectively. From the potentiodynamic curve, it shows that the  $E_{\text{corr}}$  value shifted to more negative value in the solution with an oxygen content